

Journal of Visualized Experiments

Double direct injection of blood into the cisterna magna as a model of subarachnoid hemorrhage --Manuscript Draft--

Article Type:	Methods Article - Author Produced Video
Manuscript Number:	JoVE61322R2
Full Title:	Double direct injection of blood into the cisterna magna as a model of subarachnoid hemorrhage
Section/Category:	JoVE Neuroscience
Keywords:	Subarachnoid hemorrhage; cisterna magna; mouse; vasospasm; Animal Model; sensitivo-motor test; blood
Corresponding Author:	Hélène Castel INSERM U1239, DC2N Mont Saint Aignan, FRANCE
Corresponding Author's Institution:	INSERM U1239, DC2N
Corresponding Author E-Mail:	helene.castel@univ-rouen.fr
Order of Authors:	Martin Pedard Mohamad El Amki Antoine Lefevre-Scelles Vincent Compère Hélène Castel
Additional Information:	
Question	Response
Please indicate whether this article will be Standard Access or Open Access.	Standard Access (US\$1200)



Cover letter

Dr Hélène Castel
INSERM U1239, DC2N
Team Astrocyte and Vascular Niche
Tel : +33 2 35 14 66 30
E-mail address : helene.castel@univ-rouen.fr

Rouen, France, 2020 June 19th

Ref: Revisions Required for Your JoVE Submission JoVE61322R1 -
[EMID:191ae48cac26bd85]

Dear Dr Myers,

We are glad to resubmit a second revision of our text and video manuscript entitled “Double direct injection of blood into the cisterna magna as a model of subarachnoid hemorrhage” by Pedard *et al.* to *Journal of Visualized Experiments*. The manuscript has been revised by following the important recommendations and comments from the Editorial Office.

We would like to thank you for taking this manuscript into consideration for publication to *Journal of Visualized Experiments*,

Sincerely yours,

Dr Hélène Castel
(PhD) DR2 Inserm researcher
Head of the Team Astrocyte and Vascular Niche team, Co-head of the Cancer and cognition

1 TITLE:

2 Double Direct Injection of Blood into the Cisterna Magna as a Model of Subarachnoid
3 Hemorrhage

5 AUTHORS & AFFILIATIONS:

6 Martin Pedard¹, Mohamad El Amki¹, Antoine Lefevre-Scelles^{1,2}, Vincent Compère^{1,2}, Hélène
7 Castel¹

8
9 ¹Normandie Univ, UNIROUEN, INSERM U1239, DC2N, Rouen, France, Institute for Research and
10 Innovation in Biomedicine (IRIB), Rouen, France

11 ²Department of Anesthesiology and Critical Care, Rouen University Hospital, France

12
13 Corresponding author:

14 Hélène Castel

15 helene.castel@univ-rouen.fr

16
17 Co-authors

18 Martin Pedard (martin.pedard@univ-rouen.fr)

19 Mohamad El Amki (Mohamad.ElAmki@usz.ch)

20 Antoine Lefevre-Scelles (antoine.lefevre-scelles@hotmail.fr)

21 Vincent Compère (vincent.compere@chu-rouen.fr)

23 KEYWORDS:

24 Subarachnoid hemorrhage, cisterna magna, mouse, vasospasm, animal model, sensitivo-motor
25 test, blood

27 SUMMARY:

28 We described in this protocol a standardized subarachnoid hemorrhage (SAH) mouse model by
29 a double injection of autologous whole-blood into the cisterna magna. The high degree
30 of standardization of the double-injection procedure represents a middle-to-acute
31 model of SAH with relative safety regarding mortality.

33 ABSTRACT:

34 Among strokes, subarachnoid hemorrhage (SAH) consecutive to the rupture of a cerebral
35 arterial aneurysm represents 5-9% but is responsible for about 30% of the total stroke-related
36 mortality with an important morbidity in terms of neurological outcome. A delayed cerebral
37 vasospasm (CVS) may occur most often in association with a delayed cerebral ischemia.
38 Different animal models of SAH are now being used including endovascular perforation and
39 direct injection of blood into the cisterna magna or even the prechiasmatic cistern, each
40 exhibiting distinct advantages and disadvantages. In this article, a standardized mouse model of
41 SAH by double direct injection of determined volumes of autologous whole blood into the
42 cisterna magna is presented. Briefly, mice were weighed and then anesthetized by isoflurane
43 inhalation. Then, the animal was placed in a reclining position on a heated blanket maintaining
44 a rectal temperature of 37 °C and positioned in a stereotactic frame with a cervical bend of

45 about 30°. Once in place, the tip of an elongated glass micropipette filled with the homologous
46 arterial blood taken from carotid artery of another mouse of the same age and gender
47 (C57Bl/6J) was positioned at a right angle in contact with the atlanto-occipital membrane by
48 means of a micromanipulator. Then 60 µL of blood was injected in the cisterna magna followed
49 by a 30° downward tilt of the animal for 2 minutes. The second infusion of 30 µL of blood into
50 the cisterna magna was performed 24 h after the first one. The individual follow-up of each
51 animal is carried out daily (careful evaluation of weight and well-being). This procedure allows a
52 predictable and highly reproducible distribution of blood, likely accompanied by intracranial
53 pressure elevation that can be mimicked by an equivalent injection of an artificial cerebral
54 spinal fluid (CSF), and represents an acute to mild-model of SAH inducing low mortality.

55

56 **INTRODUCTION:**

57 Subarachnoid hemorrhage (SAH) accounts for up to 5% of all stroke cases and constitutes a
58 relatively common pathology with an incidence of 7.2 to 9 patients per 100,000 per year, with a
59 mortality rate of 20%-60% depending on the study¹⁻³. In the acute phase, the mortality is
60 attributable to the severity of bleeding, rebleeding, cerebral vasospasm (CVS) and/or medical
61 complications⁴. In survivors, early brain injury (EBI) is associated with parenchymal extension of
62 hemorrhage and abrupt increase in intracranial pressure, which may result in primary cerebral
63 ischemia⁵ and immediate death in about 10%-15% of cases⁶. After the initial "acute" stage of
64 SAH, the prognosis depends on the occurrence of "secondary" or delayed cerebral ischemia
65 (DCI), detected in nearly 40% of patients by cerebral computed tomography, and in up to 80%
66 of patients after magnetic resonance imaging (MRI)^{7,8}. In addition to the CVS occurring between
67 4 to 21 days after aneurysm rupture in a majority of SAH patients, DCI⁹ may result from
68 multifactorial diffuse brain lesions secondary to microthrombosis formation, reduced cerebral
69 perfusion, neuroinflammation, and cortical spreading depression (CSD)¹⁰⁻¹³. This affects 30% of
70 SAH survivors and impacts cognitive functions including visual memory, verbal memory,
71 reaction time, and executive, visuospatial and language functions¹⁴ impairing daily life¹⁵.
72 Current standard therapies to prevent CVS and/or the poor cognitive outcomes in SAH patients
73 are based on the blockage of Ca²⁺ signaling and vasoconstriction by using Ca²⁺ channel
74 inhibitors as Nimodipine. However, more recent clinical trials targeting vasoconstriction
75 revealed dissociation between patient's neurological outcome and prevention of CVS¹⁶,
76 suggesting more complex pathophysiological mechanisms involved in SAH-long-term
77 consequences. Therefore, there is a medical need for greater understanding of the number of
78 pathological events accompanying SAH and the development of valid and standardized animal
79 models to test original therapeutic interventions.

80

81 The rupture of an intracranial aneurysm mostly responsible for SAH in humans is likely difficult
82 to mimic in preclinical animal models. Currently, the aneurysm rupture and SAH situation can
83 tentatively be tested by the perforation of the middle cerebral artery (endovascular puncture
84 model) responsible for CVS and sensitivomotor dysfunctions in mice^{17,18}. Due to the lack of any
85 possible control over the onset of bleeding and the diffusion of blood in this model, other
86 methods have been developed in rodents to generate SAH models without endovascular
87 rupture. More precisely, they consist of the direct administration of arterial blood into the
88 subarachnoid space through a single or a double injection in the magna cisterna¹⁹ or a single

89 injection into the prechiasmatic cistern²⁰. The main advantage of these mouse models without
90 endovascular rupture is the possibility to reproducibly master the surgical procedure and the
91 quality and quantity of the injected blood sample. Another advantage of this model over the
92 model by endovascular perforation in particular is the preservation of the general well-being of
93 the animal. As a matter of fact, this surgery is less invasive and technically less challenging than
94 that required to generate a carotid wall rupture. In this last model, the animal has to be
95 intubated and mechanically ventilated, while a monofilament is inserted in the external carotid
96 artery, and advanced into the internal carotid artery. This likely leads to transient ischemia due
97 to vessel obstruction by the wire path. Consequently, the co-morbidity (moribund state,
98 important pain and death) associated with surgery is less important in double injection model
99 compared with endovascular perforation model. In addition to being a more consistent SAH,
100 the double direct injection method complies with the animal welfare in research and testing
101 (reduced time under anesthesia, pain from tissue disruption in surgery and distress) and leads
102 to a minimum total number of animals used for the protocol study and personnel training.

103
104 Moreover, this allows implementation of the same protocol to transgenic mice, leading to an
105 optimized pathological understanding of the SAH and the possibility of comparative testing of
106 potential therapeutic compounds. Here, we present a standardized mouse model of
107 subarachnoid hemorrhage (SAH) by a double daily consecutive injection of autologous arterial
108 blood into the cisterna magna in 6-8 weeks-old male C57Bl/6J mice. The main advantage of this
109 model is the control of the bleeding volume compared with the endovascular perforation
110 model, and the reinforcing of the bleeding event without a drastic increase of intracranial
111 pressure²¹. Recently, the double direct injection of blood into the cisterna magna has been well
112 described on the experimental and physiopathological issues in mice. Indeed, we recently
113 demonstrated CVS of large cerebral arteries (basilar (BA), middle (MCA) and anterior (ACA)
114 cerebral arteries), cerebrovascular fibrin deposition and cell apoptosis from day 3 (D3) to 10
115 (D10), circulation defects of paravascular cerebrospinal fluid accompanied by altered
116 sensitivomotor and cognitive functions in mice, 10 days post-SAH in this model²². Thus, it makes
117 this model mastered, validated and characterized for short-term and long-lasting events post-
118 SAH. It should be ideally suitable for prospective identification of new targets and for studies on
119 potent and efficient therapeutic strategies against SAH-associated complications.

120 121 **PROTOCOL:**

122
123 All procedures were performed under the supervision of H. Castel in accordance with the
124 French Ethical Committee and guidelines of European Parliament Directive 2010/63/EU and the
125 Council for the Protection of Animals Used for Scientific Purposes. This project was approved by
126 the local CENOMEXA and the national ethic committees on animal research and testing. Male
127 C57Bl/6J Rj mice (Janvier), aged 8–12 weeks, were housed under controlled standard
128 environmental conditions: 22 °C ± 1 °C, 12 hours/12 hours light/dark cycle, and water and food
129 available ad libitum.

130 131 **1. Setup of SAH surgery and preparation for injection**

132

133 1.1 Before the beginning of surgery, pull an adequate number of glass capillaries by using a
134 micropipette puller. The injection pipette should exhibit an inner diameter of 0.86 mm and
135 outer diameter of 1.5 mm.

136

137 1.2 Prepare the artificial cerebrospinal fluid (aCSF) for the sham condition.

138

139 1.2.1 Prepare a solution with 119 mM NaCl, 2.5 mM KCl, 1 mM NaH₂PO₄, 1.3 mM MgCl₂, 10
140 mM glucose, 26.2 mM NaHCO₃ in H₂O, pH 7.4.

141

142 1.2.2 Gas aCSF with 95% O₂ and 5% CO₂ for 15 min, and then add 2.5 mM CaCl₂.

143

144 1.2.3 Sterilize the oxygenated aCSF with a 0.22 µm filter apparatus. The aCSF solution can be
145 stable for 3-4 weeks at 4 °C. If contamination (solution becoming cloudy) or a deposit formation
146 has appeared, discard and make fresh aCSF.

147

148 1.3 Collection of blood from a homologous mouse donor

149

150 1.3.1 Isolate the carotid artery along the trachea and collect the maximum amount of blood
151 by puncture of the carotid artery.

152

153 1.3.2 In practice, place the mouse into an anesthesia chamber and load the chamber with 5%
154 isoflurane until the animal loses consciousness.

155

156 1.3.3 Check the lack of reflexes by clamping one of two hind limbs to allow the setting of the
157 surgical experimental procedure.

158

159 1.3.4 Coat a 1 mL syringe with a heparin solution by using a 26 G needle (heparin sodium).
160 This will prevent blood coagulation during the next steps.

161

162 1.3.5 Install the animal positioned in dorsal decubitus with legs apart, and the nose in an
163 anesthesia mask (anesthesia maintenance with 2 to 2.5% isoflurane).

164

165 1.3.6 Isolate the carotid artery along the trachea by dissecting the omohyoid muscle
166 longitudinally. Once artery isolated, insert the needle towards the heart with the help of the
167 microdissecting hook and forceps and collect the maximum of blood via puncture of the carotid
168 artery (60 µL is needed per SAH mouse).

169

170 1.3.7 Sacrifice the anesthetized donor mouse immediately after blood collection by using
171 cervical dislocation.

172

173 **2. Animal (8-10-week-old C57BL/6J male mice) preparation**

174

175 2.1 Weigh each mouse precisely using an electronic balance. In the current study, mice
176 would have body weight within the range of 20 to 25 grams just before surgery.

177
178 2.2 As previously explained (see steps 1.3.2 and 1.3.3), induce anesthesia of mice to be
179 operated.
180
181 2.3 Shave the neck and the space between the ears with a suitable electric clipper.
182
183 2.4 Install the animal positioned in ventral decubitus with legs apart and the nose in an
184 anesthesia mask (anesthesia maintenance with 2 and 2.5% isoflurane) on a stereotactic frame.
185
186 2.5 Check that the mouse is sleeping and that his head is properly blocked.
187
188 2.6 Subcutaneously inject 100 μ L of buprenorphine (0.1 mg/kg) with a 26 G needle in the
189 lower back, to avoid pain after awakening.
190
191 2.7 Prevent dry eyes by using protective liquid gel and maintain an intrarectal temperature
192 of 37 °C by using an auto-regulated electric blanket.
193
194 2.8 Treat the posterior neck shaved area with an antiseptic solution (povidone-iodine or
195 chlorhexidine by using a sterile cotton road).
196
197 2.9 Pre-sterilize all instruments touching the prepared skin/subcutaneous tissue (heating to
198 200 °C for 2 hours) and handle aseptically.
199
200 **3. SAH induction**
201
202 3.1 On the first day (D-1)
203
204 3.1.1 Cut a 1 cm incision with thin scissors in the posterior neck, followed by the separation of
205 muscles along the midline to access the cisterna magna.
206
207 3.1.2 Cut the tip of the empty glass pipette with thin scissors. Then, adapt to a syringe
208 connected to a flexible silicone connector.
209
210 3.1.3 Transfer 60 μ L of blood or aCSF (for SAH or sham condition, respectively) in a 0.5 mL
211 tube using a precision micropipette.
212
213 3.1.4 Suck into the glass pipette the 60 μ L of blood for the SAH condition or 60 μ L of aCSF for
214 the sham condition.
215
216 3.1.5 For injection, install the pipette on the stereotactic frame using a ring or blue-tack and
217 slowly bring the pipette tip to the membrane at the interface with the cisterna magna.
218
219 3.1.6 Slowly insert the pipette tip through the atlanto-occipital membrane into the cisterna
220 magna, using a micro-manipulator of the stereotactic frame.

221
222 3.1.7 Connect the pipette previously filled with blood or aCSF to the syringe ready for
223 pressure induction.
224
225 3.1.8 Inject by pressing the plunger at a low rate around 10 $\mu\text{L}/\text{min}$, to avoid acute intracranial
226 pressure.
227
228 3.1.9 During injection, closely monitor the respiratory rate and the rectal temperature.
229
230 3.1.10 At the end of the injection, carefully take off the pipette via the micro-manipulator and
231 visually ensure that there is no leak during withdrawal.
232
233 3.1.11 Achieve hemostasis using an absorbable hemostat and run two sutures with braided
234 non-absorbable suturing thread.
235
236 3.1.12 Immediately after surgery, isolate and position the mouse in decline decubitus and
237 cover it with a survival blanket in an open box for the duration of recovery.
238
239 3.2 Second day of induction (D0)
240
241 3.2.1 After 24 hours, induce anesthesia (see steps 1.3.2 and 1.3.3). Subcutaneously inject 100
242 μL of buprenorphine again (0.1 mg/kg) and prevent dry eyes by using protective liquid gel (see
243 steps 2.7 and 2.8).
244
245 3.2.2 Install the animal on the stereotactic frame as the day before.
246
247 3.2.3 Carefully remove the sutures with microscissors.
248
249 3.2.4 Prepare the atlanto-occipital membrane as before and apply antiseptic preparation on
250 the shaved area of the neck with a sterile cotton rod.
251
252 3.2.5 Inject 30 μL of blood or aCSF at a low rate (see steps 3.1.2 to 3.1.8). Monitor the
253 respiratory rate and the rectal temperature.
254
255 3.2.1 At the end of the injection, carefully take off the pipette and control the absence of
256 blood leak during withdrawal.
257
258 3.2.2 Achieve hemostasis and run two sutures with braided absorbable suturing thread.
259
260 **4. Postoperative follow-up and end of the experiment**
261
262 4.1 Immediately after surgery, isolate and position the mouse in decline decubitus with a
263 survival blanket on its back in an open box during recovery.
264

265 4.2 Weigh and carefully observe daily the behavior of each mouse until sacrifice (e.g., D7 post-
266 surgery).

267
268 4.3 Among humane endpoints, a significant weight loss (>15% of the weight) is classically
269 noticed. A "hunched back" posture, slow movements, prostration, abnormal vocalizations of
270 hurt and/or significant aggressive behavior are also important signs of animal suffering. If any of
271 these signs or a combination of signs appears, the monitoring of the animal is reinforced within
272 hours of their appearance. If the animal's welfare worsens or does not improve within 48 hours,
273 it will be considered that a level of intolerable suffering is reached, and euthanasia is carried
274 out.

275
276 4.4 At the time of choice, sacrifice anesthetized mice by decapitation, and harvest brains for
277 further analyses.

278
279 4.5 Perform euthanasia (decapitation) after isoflurane anesthesia (5%).
280

281 **REPRESENTATIVE RESULTS:**

282 **Experimental timeline, procedure, follow-up and mortality**

283 **Figure 1A** and **Figure 1B** summarize the SAH model protocol by double intracisternal injection
284 of blood. Briefly, on the first day of SAH induction (D-1), 60 μ L of blood withdrawn from a
285 homologous mouse or 60 μ L of artificial cerebrospinal fluid (aCSF) were injected into the
286 cisterna magna in SAH or sham conditions, respectively. The next day (D0), 30 μ L of blood
287 withdrawn from a homologous mouse or 30 μ L of aCSF were injected into the cisterna magna in
288 SAH or Sham conditions, respectively. Twenty-four hours after surgery, mouse killing and brain
289 analysis allowed to observe the blood distribution into the paravascular spaces as illustrated in
290 **Figure 1C**. As a sensitive indicator for general welfare from D1 to sacrifice, the body weight was
291 daily assessed from the D1 to D8 and showed a significant reduced body weight gain in SAH
292 compared with sham animals from D1 to D8 (**Figure 1D**), suggesting a long-lasting recovery
293 process and prolonged pathological events post-SAH. Post-operative mortality was 26.7% at D7
294 with most animals dying on D1 or D4 after surgery (**Figure 1D**). Transcardial perfusion of Indian
295 ink at D5 enabled the observation of macroscopic CVS as illustrated in **Figure 1C**.
296

297 **Cerebral vasospasm after SAH**

298 As shown by El Amki et al.²², CVS of the basilar artery (BA), middle cerebral artery (MCA) and
299 anterior cerebral artery (ACA) was present in SAH model by double intracisternal injection of
300 blood in either ACA, MCA or BA from D3 to D10 post-surgery. Briefly (**Figure 2A**), after mouse
301 sacrifice and decapitation, brains were harvested and post-fixed in 4% paraformaldehyde (PFA),
302 and then frozen at -80 °C, before being sliced into 20 μ m transversal slices using a cryostat.
303 Hematoxylin and eosin staining was performed for BA (interaural 0.40 mm; bregma -3.40 mm),
304 MCA (interaural 2.58 mm; bregma -1.22 mm) and ACA (interaural 4.90 mm; bregma 1.10 mm)
305 to allow CVS identification via systematic image acquisition of colored slices by using a
306 microscope-mounted camera. In order to evaluate the absence or the presence of macroscopic
307 CVS, the lumen area/wall thickness ratio was calculated for each stained artery. The lower is
308 the ratio, the more severe is the CVS. Thus, a CVS occurred in BA in SAH brains compared with

309 sham mouse brains (**Figure 2B**) but also in other large cerebral arteries (MCA, ACA, data not
310 shown²²).

311

312 **Sensitivomotor dysfunctions after SAH**

313 The measurement of specific motor deficits, well described in this SAH model by El Amki et al.²²
314 and Clavier et al.²³, can be considered as a main evaluation criterion of outcome to test specific
315 therapeutic targets regulating these SAH-associated long-term effects. Briefly (**Figure 3A**), at D6
316 post-surgery, each mouse was evaluated in the open-field test for 10 minutes. By means of the
317 ANY-maze software version 4.99, the distance covered and the number of rearing and leaning
318 were recorded. Twenty-four hours after the open-field test, each mouse took part in three
319 successive sessions of the beam walking test involving, after a device habituation period, the
320 measurement of total walking time, the time to reach the platform and the number of trips.
321 Results were expressed as a mean of three sessions. As shown by El Amki et al.²²,
322 sensitivomotor dysfunctions evaluated by the beam walking test at D10 post-surgery were
323 shown to be present in the SAH model (**Figure 3B**). At D9, spontaneous activity of mice
324 evaluated by the open-field test during 10 minutes, was also significantly affected by SAH as
325 detected by the distance crossed and the vertical activity compared with the sham condition
326 (**Figure 3C**).

327

328 **FIGURE AND TABLE LEGENDS:**

329

330 **Figure 1. Experimental design, surgical procedure, blood distribution, macroscopic**
331 **vasospasm, body weight and mortality after SAH.** (A) Schematic diagram showing the
332 experimental design of this protocol. D-1 and D0 represent the days of surgery with a double
333 injection of 60 and 30 μ L of aCSF (Sham) or blood (SAH) into the cisterna magna, respectively.
334 From D1 to D8, mice were daily observed and weighed. At D1, brains were harvested to
335 observe the blood distribution into paravascular spaces (C). The D6 and D7 were chosen as
336 optimized time window for behavioral analyses including open field and beam walking tests. At
337 D8, brains were sampled to evaluate CVS, as shown macroscopically in (C). (B) Surgical
338 procedure of blood injection into the cisterna magna. Blood was collected from carotid artery
339 of a homologous mouse. After animal preparation and installation on stereotactic frame, a
340 nape incision was carried out in the posterior neck, the posterior muscles were separated, and
341 then the underlying muscles were dissected to open an access to the vascularized membrane
342 delimitating the cisterna magna. The pipette was inserted into the cisterna magna before blood
343 injection. (C) Illustration of the blood distribution into paravascular spaces twenty-four hours
344 after surgery and of macroscopic CVS after transcatheter perfusion of Indian ink five days after
345 surgery in SAH compared with Sham condition. (D) Weight evolution from D-1 to D8 post-
346 surgery in Sham (n=10) and SAH C57Bl/6J (n=15) mice. SAH mice showed a decrease in
347 percentage of body weight gain from D1 to D8 compared with the sham mice ($p<0.01$). ANOVA
348 with Bonferroni's post hoc test for multiple comparison tests. Survival curve following surgery
349 in sham (n=10) and SAH C57Bl/6J (n=15) mice. Data were expressed as Kaplan Meier curves.
350 SAH mice showed a more important mortality at D7 post-surgery compared with sham mice
351 ($p<0.05$). Mantel-Cox test.

352

353 **Figure 2. Experimental design for cerebral vasospasm analysis and time course of cerebral**
354 **vasospasm in basilar artery after SAH. (A)** Schematic diagram showing the experimental design
355 of protocol for CVS quantification. After post-fixation by 4%PFA, frozen brains were serially
356 sliced using a cryostat into 20 μ m transversal slices on gelatin-coated glass slides. Hematoxylin
357 and Eosin (H&E) staining was performed from brain slices bearing ACA, MCA and BA.
358 Microphotographies were acquired using a microscope-mounted camera at a 200x
359 magnification. Lumen area and vessel wall thickness were quantified using ImageJ by a simple
360 blind method. **(B)** Time course of CVS in BA after SAH. Representative microphotographies of
361 H&E staining showing BA morphology (lumen area and wall thickness) in sham and SAH brain
362 slices at D7 post-SAH. Quantification histograms of lumen area/wall thickness ratio showing
363 CVS in the BA from D3 to D10 post-surgery (*, $p < 0.05$). Data were expressed as mean \pm SEM.
364 $n = 6$ /condition. ANOVA with Bonferroni's post hoc test for multiple comparisons.

365
366 **Figure 3. Experimental design for behavioral analysis of long-term sensitivomotor deficits**
367 **after SAH. (A)** Schematic diagram showing the experimental design of the behavioral analysis
368 protocol after SAH. Briefly, at D6 post-surgery, motor activity behavior of mice was evaluated
369 by an open-field test for 10 minutes, in which covered distance and the number of rearing and
370 leaning was recorded. After a 24 h rest period, the sensitivomotor behavior of mice was
371 evaluated by the beam walking test, in which the walking time, the time to reach the platform
372 and the number of trips were recorded. **(B)** From El Amki et al.²²: In the beam walking test, SAH
373 mice showed increased number of trips compared with controls at D7 (**, $p < 0.01$), D10 (***,
374 $p < 0.001$) and D14 (*, $p < 0.05$) and with sham mice at D10 (*, $p < 0.05$). **(C)** From El Amki et al.²²:
375 SAH mice exhibited a decreased distance crossed (*, $p < 0.05$) and vertical activity compared
376 with Sham mice at D9 (*, $p < 0.01$). ANOVA followed by Sidak's multiple comparisons test. Data
377 were expressed as mean \pm SEM. $n = 10-12$ /condition.

378 379 **DISCUSSION:**

380 Despite the intensity of the research in the field of SAH and the development of therapeutic
381 strategies such as endovascular and pharmacological treatment options increasing over the
382 past twenty years, mortality remains high within the first week of hospital admission and
383 reaches about 50% during the following 6 months^{24,25}. This current preclinical model by daily
384 double injection of homologous arterial blood into the cisterna magna has been recognized for
385 its validity and its association with a low mortality rate. Indeed, among SAH rodent models, a
386 wide range of mortality rates has been reported: 0-16% mortality with single blood injection
387 into cisterna magna²⁶⁻³⁵, 10-33% mortality with blood injection into prechiasmatic
388 cistern^{20,27,36,37}, 16-66% mortality in the model by endovascular perforation³⁸⁻⁴⁵ and 0-43% with
389 the model by double blood injection into cisterna magna^{34,35,46-48}. The low mortality rate in the
390 model (9% or 27%, depending on the age of mice) can result from the weak amount of blood
391 injected, the slow-duration of injection, and the tilting of the animal avoiding localized pressure
392 on the brainstem, compared with other double injection models. In SAH patients, the window
393 of CVS occurrence is classically detected at D4-D10 post-hemorrhage. However, in animals, the
394 time to onset and the duration of CVS are less studied and may vary between HSA models,
395 likely depending on experimental protocols and animal species²¹.

396

397 In this context, the model here resembles clinical SAH physiopathology in terms of SAH-
398 associated CVS. In general, in endovascular perforation model, CVS occurs in the MCA and BA
399 after 1 hour in rats⁴⁰ and after 3 days in mice¹⁷. In the model by blood injection into
400 prechiasmatic cistern, CVS occurrence was shown between two⁴⁹ and eight days³⁷ in rats. In the
401 model of double injection into cisterna magna in rats, CVS develops between 10 minutes²⁹ and
402 3 days³¹. We are the first to describe kinetic of appearance of CVS in a mouse model of SAH by
403 double injection, establishing CVS in main cerebral arteries (ACA, MCA and BA) since 3 days and
404 being sustained until the 10th day post-SAH²², close to what is observed in SAH patients. This
405 last model could be defined as a skilled model of SAH, severe enough without mortality,
406 allowing investigation of mechanisms and therapeutics targeting CVS.

407
408 However, this mouse SAH model may also present some limits. The first point is the lack of
409 vessel wall rupture, as possibly reproduced in the collagenase-induced SAH model, through
410 destruction/digestion of blood vessel basal lamina⁵⁰. As for the occurrence of macroscopic CVS,
411 reduced cerebral blood flow (CBF) in some brain territories is not systematically correlated with
412 neurological outcome, thus CBF should be evaluated in this proposed model of SAH. Previous
413 rat studies using Laser Doppler Flowmetry in a SAH model of double injection demonstrated the
414 CBF acute decrease to 30–52% from baseline after the first injection, with a return to baseline
415 after 2 to 3 days post-injection⁵¹⁻⁵³. In agreement, it has been shown by MRI a decrease of CBF
416 of 33-50% at D3 and 27–44% at D5 after SAH induction in rat double injection models^{54,55}. The
417 double injection into the cisterna magna allows for a predictable distribution of blood along the
418 subarachnoid space, resulting especially in blood clots around the posterior circulation, but can
419 introduce variations in physiological parameters. To avoid intracranial pressure (ICP) from rising
420 with the volume of injected blood entering into the spinal canal, both leading to confounding
421 functional impairments⁵⁶, the choice to remove an equivalent volume of cerebrospinal fluid
422 could be done, as previously done in other models^{30,51}. In the model here, sham mice received
423 an equivalent volume of aCSF or physiological 0.9% NaCl, depending on the experiment,
424 obviously leading to a rising of ICP. Thus, an acute increase of ICP results in an increase from 18
425 mmHg to 120 mmHg^{27,48,53} in the single injection of blood in the cisterna magna model, from 46
426 to 107 mmHg^{27,37,49} in the prechiasmatic cistern blood injection model, and from 27 to 110
427 mmHg^{39,40,53,57,58} in the endovascular perforation model. In contrast, the double blood injection
428 into cisterna magna was associated with a smaller ICP increase from 60 to 67 mmHg^{48,53}.
429 Moreover, the action of removing CSF would also alter ICP and modify CSF. In the SAH model
430 here, the decision was to not remove CSF before blood injection but to accompany surgery by a
431 procedure consisting in tilting the animal head from 30°. The aim is to attenuate ICP by
432 allowing the blood distribution into the anterior circulation, an important and necessary step to
433 mimic human SAH physiopathology. In SAH patients, a sharp rise in ICP is detected and is
434 associated with a transient global cerebral ischemia⁵⁹, likely contributing to a sustained
435 impairment of autoregulation and early neuronal cell loss⁶⁰. However, after the first event post-
436 SAH, an early external ventricular drainage is often adopted for concerned SAH patients, to
437 avoid brain swelling and hydrocephalus⁶¹. Here, the double injection SAH model may not be
438 severe at the first bleeding event to provoke the ICP-dependent consequences observed in
439 patients, but likely reproduce a sustained and mild enhanced ICP for days post-SAH.

440

441 In addition, another uncontrolled parameter in the SAH model here was the potential variations
442 of the mean arterial blood pressure (MABP) induced by excessively rapid blood injection
443 procedure²⁷. Indeed, MABP typically acutely rises after experimental SAH to preserve cerebral
444 perfusion pressure and thereafter, falls to baseline. In the SAH model here, we injected blood
445 or aCSF (~ 10 µL/min) at a low rate to avoid these MABP variations. Regarding the
446 neurobiological events in this model mimicking those observed in humans, we previously
447 showed that the double blood injection model of SAH induces long-lasting CVS,
448 microthrombosis formation and cerebral brain damage including defect in potential
449 paravascular diffusion from day 3 to day 10 post-SAH²². However, recent data describing that
450 CSD is involved in SAH-associated DCI¹³ strongly support the pursuit of this type of
451 investigations in the mouse model of double injection. This should enable scientific
452 breakthroughs on the beneficial impact of new therapies targeting CSD.

453

454 To conclude, the model of double injection of whole arterial blood into the cisterna magna is a
455 mastered model that allows an easy way to mimic the human SAH physiopathology including
456 CVS, microthrombosis, vascular inflammation, neurological deficits and mortality rate. It
457 represents a validated model for testing novel therapeutic approaches to treat SAH-associated
458 morbi-mortality.

459

460 **ACKNOWLEDGMENTS:**

461 We thank the PRIMACEN platform (Normandie Rouen University, France) for imaging
462 equipment and Mr. Arnaud Arabo, Mrs Julie Maucotel and Mrs Martine Dubois, for animal
463 housing and care. We thank Mrs. Celeste Nicola for lending her voice to the videotaping of the
464 protocol. This work was supported by Seinari Normandy maturation program, Fondation AVC
465 under the aegis of the FRM, Normandie Rouen University and Inserm. The Normandy Region
466 and the European Union (3R project). Europe gets involved in Normandy with European
467 Regional Development Fund (ERDF).

468

469 **DISCLOSURES:**

470 The authors have nothing to disclose.

471

472 **REFERENCES**

473 1 Rincon, F., Rossenwasser, R. H., Dumont, A. The epidemiology of admissions of
474 nontraumatic subarachnoid hemorrhage in the United States. *Neurosurgery*. **73** (2), 217-222,
475 212-213 (2013).

476 2 Sandvei, M. S. et al. Incidence and mortality of aneurysmal subarachnoid hemorrhage in
477 two Norwegian cohorts, 1984-2007. *Neurology*. **77** (20), 1833-1839 (2011).

478 3 van Gijn, J., Kerr, R. S., Rinkel, G. J. Subarachnoid haemorrhage. *Lancet*. **369** (9558), 306-
479 318 (2007).

480 4 Solenski, N. J. et al. Medical complications of aneurysmal subarachnoid hemorrhage: a
481 report of the multicenter, cooperative aneurysm study. Participants of the Multicenter
482 Cooperative Aneurysm Study. *Critical Care Medicine*. **23** (6), 1007-1017 (1995).

483 5 Cahill, J., Calvert, J. W., Zhang, J. H. Mechanisms of early brain injury after subarachnoid
484 hemorrhage. *Journal of Cerebral Blood Flow & Metabolism*. **26** (11), 1341-1353 (2006).

485 6 Huang, J., van Gelder, J. M. The probability of sudden death from rupture of intracranial
486 aneurysms: a meta-analysis. *Neurosurgery*. **51** (5), 1101-1105; 1105-1107 (2002).

487 7 Rabinstein, A. A. Secondary brain injury after aneurysmal subarachnoid haemorrhage:
488 more than vasospasm. *Lancet Neurology*. **10** (7), 593-595 (2011).

489 8 Kivisaari, R. P. et al. MR Imaging After Aneurysmal Subarachnoid Hemorrhage and
490 Surgery: A Long-term Follow-up Study. *American Journal of Neuroradiology*. **22** (6), 1143-1148
491 (2001).

492 9 Mayberg, M. R. et al. Guidelines for the management of aneurysmal subarachnoid
493 hemorrhage. A statement for healthcare professionals from a special writing group of the
494 Stroke Council, American Heart Association. *Stroke*. **25** (11), 2315-2328 (1994).

495 10 Dankbaar, J. W. et al. Relationship between vasospasm, cerebral perfusion, and delayed
496 cerebral ischemia after aneurysmal subarachnoid hemorrhage. *Neuroradiology*. **51** (12), 813-
497 819 (2009).

498 11 Sehba, F. A., Hou, J., Pluta, R. M., Zhang, J. H. The importance of early brain injury after
499 subarachnoid hemorrhage. *Progress in Neurobiology*. **97** (1), 14-37 (2012).

500 12 Miller, B. A., Turan, N. Inflammation, vasospasm, and brain injury after subarachnoid
501 hemorrhage. **2014**, 384342 (2014).

502 13 Dreier, J. P. et al. Delayed ischaemic neurological deficits after subarachnoid
503 haemorrhage are associated with clusters of spreading depolarizations. *Brain*. **129** (Pt 12),
504 3224-3237 (2006).

505 14 Mayer, S. et al. Global and domain-specific cognitive impairment and outcome after
506 subarachnoid hemorrhage. *Neurology*. **59** (11), 1750-1758 (2002).

507 15 Al-Khindi, T., Macdonald, R. L., Schweizer, T. A. Cognitive and functional outcome after
508 aneurysmal subarachnoid hemorrhage. *Stroke*. **41** (8), e519-e536 (2010).

509 16 Macdonald, R. L. et al. Randomized trial of clazosentan in patients with aneurysmal
510 subarachnoid hemorrhage undergoing endovascular coiling. *Stroke*. **43** (6), 1463-1469 (2012).

511 17 Parra, A. et al. Mouse model of subarachnoid hemorrhage associated cerebral
512 vasospasm: methodological analysis. *Neurological Research*. **24** (5), 510-516 (2002).

513 18 Schuller, K., Buhler, D., Plesnila, N. A murine model of subarachnoid hemorrhage.
514 *Journal of Visualized Experiments*. (81), e50845 (2013).

515 19 Lin, C. L. et al. A murine model of subarachnoid hemorrhage-induced cerebral
516 vasospasm. *Journal of Neuroscience Methods*. **123** (1), 89-97 (2003).

517 20 Sabri, M. et al. Anterior circulation mouse model of subarachnoid hemorrhage. *Brain*
518 *Research*. **1295**, 179-185 (2009).

519 21 Leclerc, J. L. et al. A Comparison of Pathophysiology in Humans and Rodent Models of
520 Subarachnoid Hemorrhage. *Frontiers in Molecular Neuroscience*. **11** 71 (2018).

521 22 El Amki, M. et al. Long-Lasting Cerebral Vasospasm, Microthrombosis, Apoptosis and
522 Paravascular Alterations Associated with Neurological Deficits in a Mouse Model of
523 Subarachnoid Hemorrhage. *Molecular Neurobiology*. **55** (4), 2763-2779 (2018).

524 23 Clavier, T. et al. Association between vasoactive peptide urotensin II in plasma and
525 cerebral vasospasm after aneurysmal subarachnoid hemorrhage: a potential therapeutic target.
526 *Journal of Neurosurgery*. 1-11 (2018).

527 24 Kundra, S., Mahendru, V., Gupta, V., Choudhary, A. K. Principles of neuroanesthesia in
528 aneurysmal subarachnoid hemorrhage. *Journal of Anaesthesiology Clinical Pharmacology*. **30**

529 (3), 328-337 (2014).

530 25 Schertz, M. et al. Incidence and Mortality of Spontaneous Subarachnoid Hemorrhage in
531 Martinique. *PLOS ONE*. **11** (5), e0155945 (2016).

532 26 Lin, C.-L. et al. A murine model of subarachnoid hemorrhage-induced cerebral
533 vasospasm. *Journal of Neuroscience Methods*. **123** (1), 89-97 (2003).

534 27 Prunell, G. F., Mathiesen, T., Diemer, N. H., Svendgaard, N.-A. Experimental
535 subarachnoid hemorrhage: subarachnoid blood volume, mortality rate, neuronal death,
536 cerebral blood flow, and perfusion pressure in three different rat models. *Neurosurgery*. **52** (1),
537 165-176 (2003).

538 28 Turowski, B. et al. New angiographic measurement tool for analysis of small cerebral
539 vessels: application to a subarachnoid haemorrhage model in the rat. *Neuroradiology*. **49** (2),
540 129-137 (2007).

541 29 Boyko, M. et al. The neuro-behavioral profile in rats after subarachnoid hemorrhage.
542 *Brain Research*. **1491**, 109-116 (2013).

543 30 Muñoz-Sánchez, M. Á. et al. Urotensinergic system genes in experimental subarachnoid
544 hemorrhage. *Medicina Intensiva (English Edition)*. **41** (8), 468-474 (2017).

545 31 Delgado, T., Brismar, J., Svendgaard, N. A. Subarachnoid haemorrhage in the rat:
546 angiography and fluorescence microscopy of the major cerebral arteries. *Stroke*. **16** (4), 595-602
547 (1985).

548 32 Solomon, R. A., Antunes, J. L., Chen, R., Bland, L., Chien, S. Decrease in cerebral blood
549 flow in rats after experimental subarachnoid hemorrhage: a new animal model. *Stroke*. **16** (1),
550 58-64 (1985).

551 33 Ram, Z., Sahar, A., Hadani, M. Vasospasm due to massive subarachnoid haemorrhage—a
552 rat model. *Acta Neurochirurgica*. **110** (3-4), 181-184 (1991).

553 34 Glenn, T. C. et al. Subarachnoid hemorrhage induces dynamic changes in regional
554 cerebral metabolism in rats. *Journal of Neurotrauma*. **19** (4), 449-466 (2002).

555 35 Gules, I., Satoh, M., Clower, B. R., Nanda, A., Zhang, J. H. Comparison of three rat models
556 of cerebral vasospasm. *American Journal of Physiology-Heart and Circulatory Physiology*. **283**
557 (6), H2551-2559 (2002).

558 36 Sabri, M. et al. Mechanisms of microthrombi formation after experimental subarachnoid
559 hemorrhage. *Neuroscience*. **224**, 26-37 (2012).

560 37 Jeon, H., Ai, J., Sabri, M., Tariq, A., Macdonald, R. Learning deficits after experimental
561 subarachnoid hemorrhage in rats. *Neuroscience*. **169** (4), 1805-1814 (2010).

562 38 Silasi, G., Colbourne, F. Long-term assessment of motor and cognitive behaviours in the
563 intraluminal perforation model of subarachnoid hemorrhage in rats. *Behavioural Brain*
564 *Research*. **198** (2), 380-387 (2009).

565 39 Bederson, J. B., Germano, I. M., Guarino, L. Cortical blood flow and cerebral perfusion
566 pressure in a new noncraniotomy model of subarachnoid hemorrhage in the rat. *Stroke*. **26** (6),
567 1086-1092 (1995).

568 40 Bederson, J. B. et al. Acute vasoconstriction after subarachnoid hemorrhage.
569 *Neurosurgery*. **42** (2), 352-362 (1998).

570 41 Park, I.-S. et al. Subarachnoid hemorrhage model in the rat: modification of the
571 endovascular filament model. *Journal of Neuroscience Methods*. **172** (2), 195-200 (2008).

572 42 Van den Bergh, W. et al. Magnetic resonance imaging in experimental subarachnoid

573 haemorrhage. *Acta Neurochirurgica*. **147** (9), 977-983 (2005).

574 43 Peng, J. et al. LRP1 activation attenuates white matter injury by modulating microglial
575 polarization through Shc1/PI3K/Akt pathway after subarachnoid hemorrhage in rats. *Redox*
576 *Biology*. **21**, 101121-101121 (2019).

577 44 Okada, T. et al. Selective Toll-Like Receptor 4 Antagonists Prevent Acute Blood-Brain
578 Barrier Disruption After Subarachnoid Hemorrhage in Mice. *Molecular Neurobiology*. **56** (2),
579 976-985 (2019).

580 45 Tiebosch, I. A. et al. Progression of brain lesions in relation to hyperperfusion from
581 subacute to chronic stages after experimental subarachnoid hemorrhage: a multiparametric
582 MRI study. *Cerebrovascular Diseases*. **36** (3), 167-172 (2013).

583 46 Weidauer, S., Vatter, H., Dettmann, E., Seifert, V., Zanella, F. E. Assessment of
584 vasospasm in experimental subarachnoid hemorrhage in rats by selective biplane digital
585 subtraction angiography. *Neuroradiology*. **48** (3), 176-181 (2006).

586 47 Lee, J. Y., Huang, D. L., Keep, R., Sagher, O. Characterization of an improved double
587 hemorrhage rat model for the study of delayed cerebral vasospasm. *Journal of Neuroscience*
588 *Methods*. **168** (2), 358-366 (2008).

589 48 Cai, J. et al. A novel intravital method to evaluate cerebral vasospasm in rat models of
590 subarachnoid hemorrhage: a study with synchrotron radiation angiography. *PloS one*. **7** (3),
591 e33366 (2012).

592 49 Piegras, A., Thome, C., Schmiedek, P. Characterization of an anterior circulation rat
593 subarachnoid hemorrhage model. *Stroke*. **26** (12), 2347-2352 (1995).

594 50 Rosenberg, G. A., Mun-Bryce, S., Wesley, M., Kornfeld, M. Collagenase-induced
595 intracerebral hemorrhage in rats. *Stroke*. **21** (5), 801-807 (1990).

596 51 Raslan, F. et al. A modified double injection model of cisterna magna for the study of
597 delayed cerebral vasospasm following subarachnoid hemorrhage in rats. *Experimental &*
598 *Translational Stroke Medicine*. **4** (1), 23 (2012).

599 52 Cai, J. et al. A novel intravital method to evaluate cerebral vasospasm in rat models of
600 subarachnoid hemorrhage: a study with synchrotron radiation angiography. *PLoS One*. **7** (3),
601 e33366 (2012).

602 53 Lee, J. Y., Sagher, O., Keep, R., Hua, Y., Xi, G. Comparison of experimental rat models of
603 early brain injury after subarachnoid hemorrhage. *Neurosurgery*. **65** (2), 331-343; discussion
604 343 (2009).

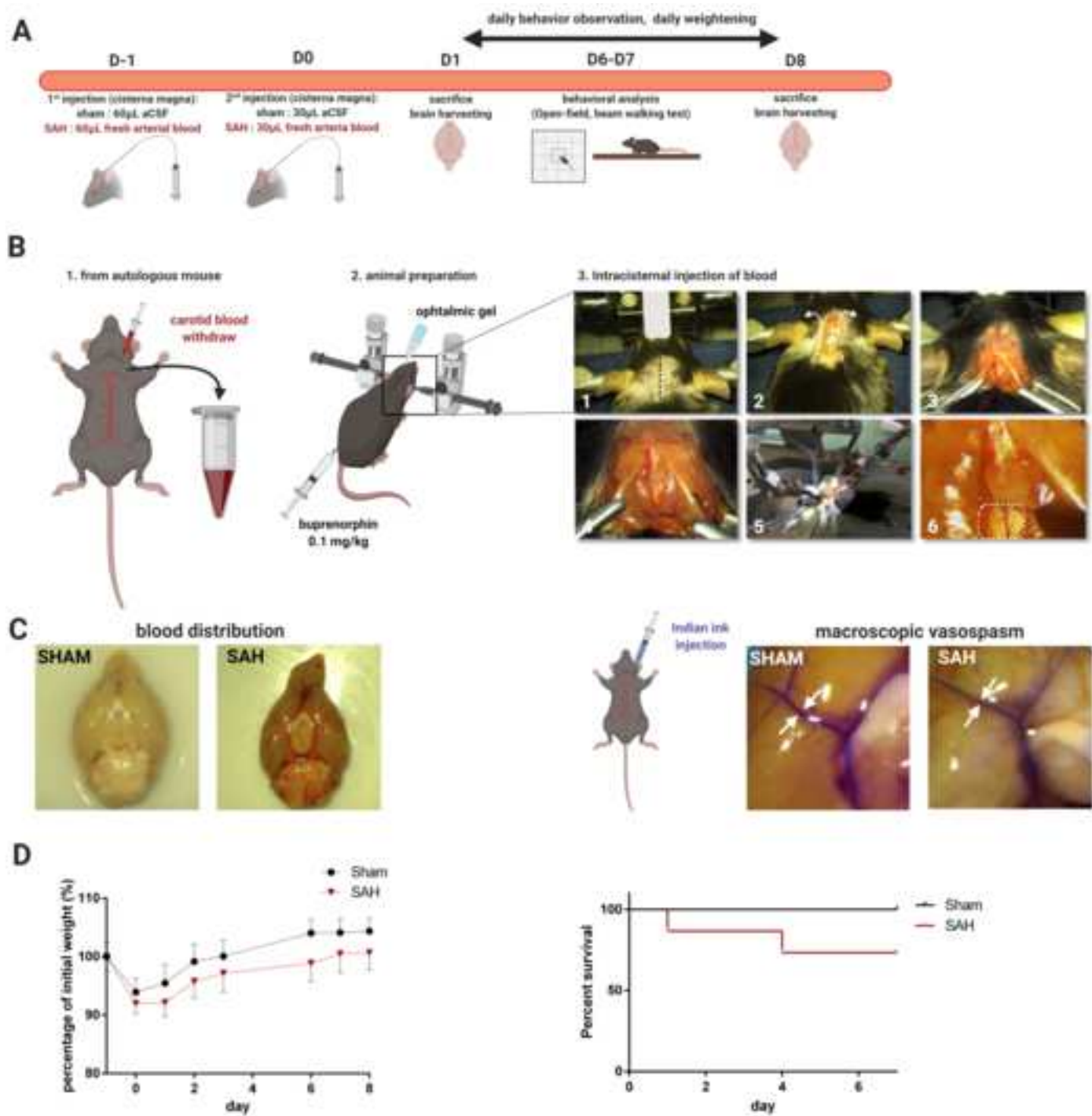
605 54 Guresir, E. et al. The effect of common carotid artery occlusion on delayed brain tissue
606 damage in the rat double subarachnoid hemorrhage model. *Acta Neurochir (Wien)*. **154** (1), 11-
607 19 (2012).

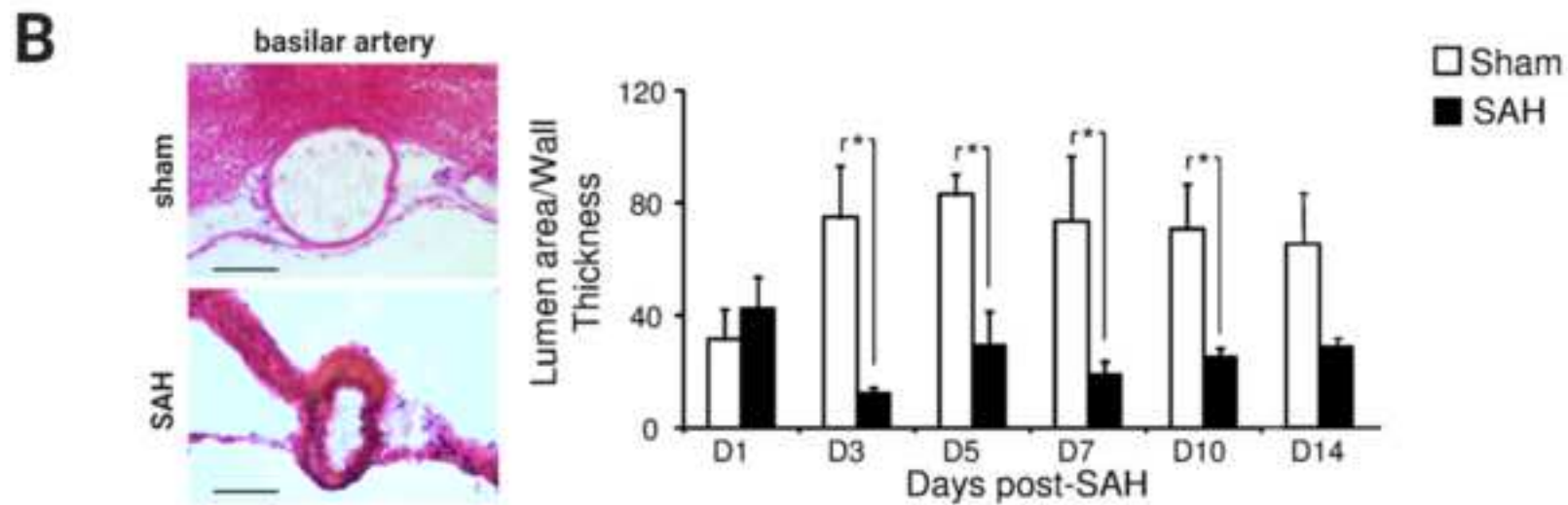
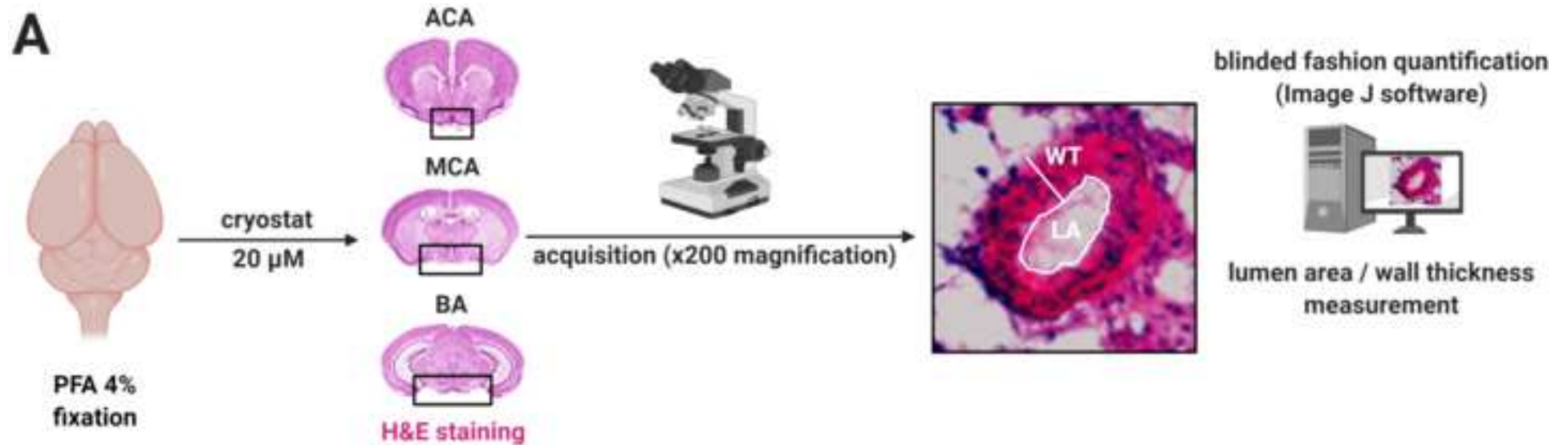
608 55 Vatter, H. et al. Time course in the development of cerebral vasospasm after
609 experimental subarachnoid hemorrhage: clinical and neuroradiological assessment of the rat
610 double hemorrhage model. *Neurosurgery*. **58** (6), 1190-1197; 1190-1197 (2006).

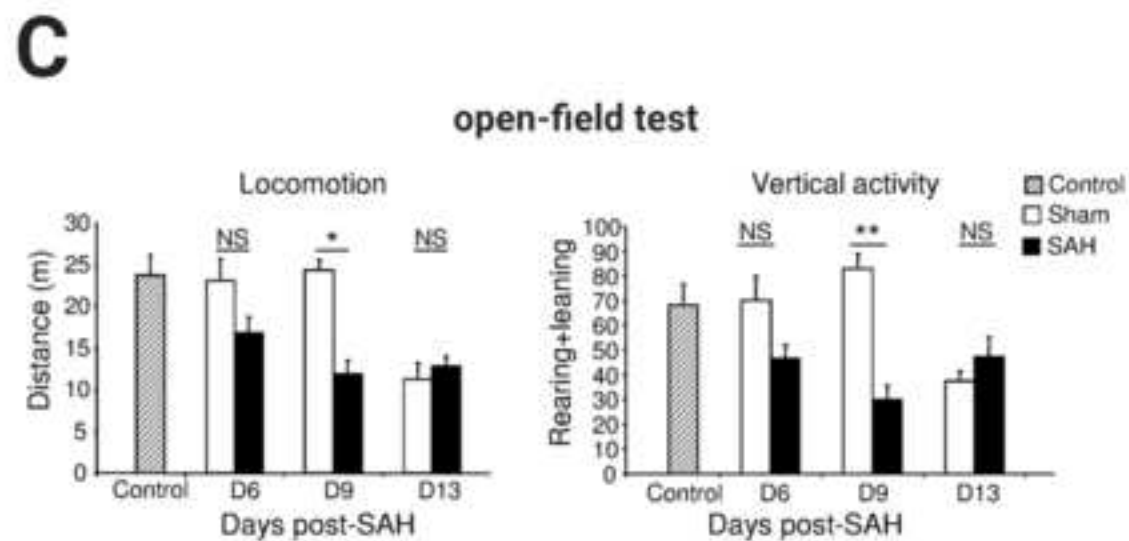
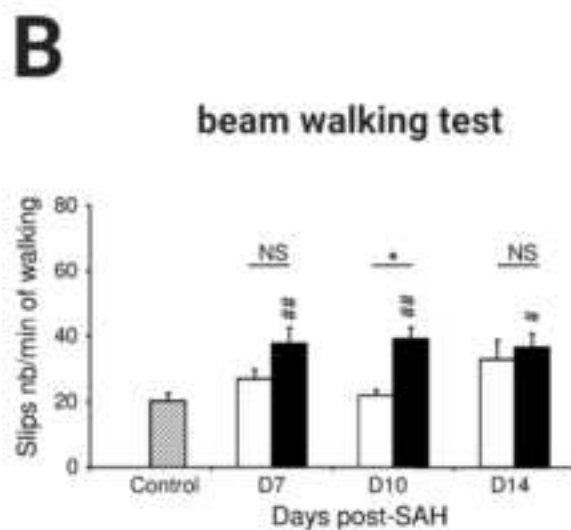
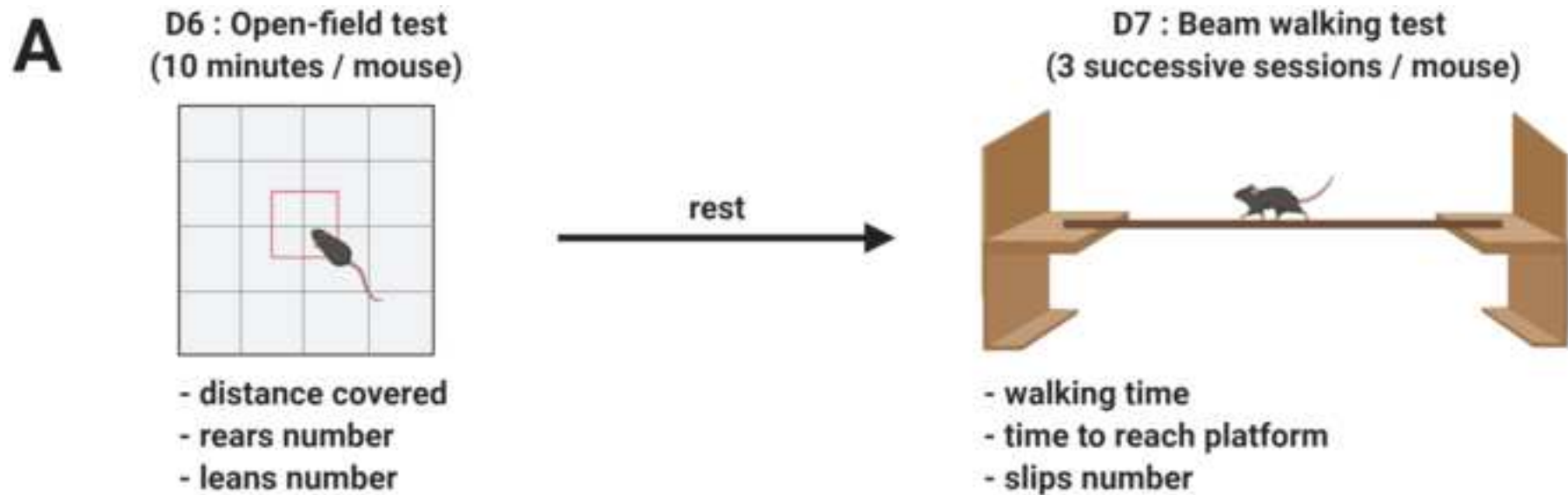
611 56 Leonardo, C. C., Robbins, S., Doré, S. Translating basic science research to clinical
612 application: models and strategies for intracerebral hemorrhage. *Frontiers in Neurology*. **3** 85
613 (2012).

614 57 Feiler, S., Friedrich, B., Schöller, K., Thal, S. C., Plesnila, N. Standardized induction of
615 subarachnoid hemorrhage in mice by intracranial pressure monitoring. *Journal of Neuroscience*
616 *Methods*. **190** (2), 164-170 (2010).

617 58 Westermaier, T., Jauss, A., Eriskat, J., Kunze, E., Roosen, K. Acute vasoconstriction:
618 decrease and recovery of cerebral blood flow after various intensities of experimental
619 subarachnoid hemorrhage in rats. *Journal of Neurosurgery*. **110** (5), 996-1002 (2009).
620 59 van Lieshout, J. H. et al. An introduction to the pathophysiology of aneurysmal
621 subarachnoid hemorrhage. *Neurosurgical Review*. **41** (4), 917-930 (2018).
622 60 Conzen, C. et al. The Acute Phase of Experimental Subarachnoid Hemorrhage:
623 Intracranial Pressure Dynamics and Their Effect on Cerebral Blood Flow and Autoregulation.
624 *Translational Stroke Research*. **10** (5), 566-582 (2019).
625 61 Connolly, E. S., Jr. et al. Guidelines for the management of aneurysmal subarachnoid
626 hemorrhage: a guideline for healthcare professionals from the American Heart
627 Association/american Stroke Association. *Stroke*. **43** (6), 1711-1737 (2012).
628







Name of Material/Equipment	Company	Catalog Number	Comments/Description
absorbable hemostat	Ethicon	Surgicel	
absorbable suturing thread	Ethicon	Vicryl 5.0	
auto-regulated electric blanket	Harvard Apparatus	50-7087-F	
bluetack for capillary fixation	UHU	Patafix	
electronic balance	Denver Instrument	MXX-2001	
glass capillaries	Harvard Apparatus	GC150F-15	inner diameter 0.86 mm
isoflurane vaporizer	Phymep	V100	outer diameter 1.5 mm
micropipette puller	Sutter Instrument Company	P-97	
needle 26 G	BD microbalance	300300	
non absorbable suturing thread	Peters surgical	Filapeau 4.0	
stereotaxic frame	David Kopf instruments	Model 902	
surgical equipment	Kent scientific	clamp, microscissors, thin scissors	
syringe 20 mL TERUMO	Thermofisher	11866071	

Response to Editor comments for Journal of Visualized Experiments

Ref: Revisions Required for Your JoVE Submission JoVE61322R1 - [EMID:191ae48cac26bd85]

Dear Dr Myers,

We would like to thank you and the reviewers for comments on the revised manuscript that have contributed to improve the quality of our work. We remain of course at your disposal if any further clarifications are required.

Sincerely yours,
Hélène Castel

Response to editorial and production comments:

Concern 1: *There continues to be many phrases throughout the manuscript that are awkward or not clear. Please employ professional copy-editing services.*

We apologize for this lack of caution. We made substantial modifications highlighted in yellow in the revised manuscript to correct the english speaking errors and the lack of meaning in some sentences.

Concern 2: *Chapter Title Cards: Please allow enough time for the chapter title cards to be read- consider adding 1 or 2 more seconds of duration to the chapter title cards, and standardize the duration across the chapter title cards.*

We added 2 seconds of duration for each chapter title cards. Moreover, this duration has been standardized across all chapter title cards.

Concern 3: *3:39 - Please revise to "Mouse weighing 20-25 grams". Weightening is not a word.*

This error has been corrected in the new version of video (see 3:36-3:40 in new version).

Concern 4: *6:44 - Please revise to "0.1 mg/kg" instead of 0,1 mg/*

This error has been corrected in the new version of the video (see at 4:01 and 06:47 in new version).

Concern 5: *Audio narration : 3:33 - Weigh each mouse, not weight each mouse.*

We recorded a new sequence to correct audio narration (listen at 3:31 in new version).

Concern 6: *Jump Cuts: 06:07 Please use a dissolve transition here instead of the jump cut. 07:20 Please use a dissolve or fade transition here instead of a jump cut.*

We changed jump cuts by a dissolve transition at 06:07 and 07:24 in the new version of video.

Concern 7: *Animal Anesthesia: 02:58 - 03:09 Please eliminate the shot of the isoflurane chamber, as we don't allow shots of initial anesthetization. You can include the toe pinch test and onward, and the verbal or textual description of the anesthetic regimine is allowed to be presented.*

The part in which we saw the shot of the isoflurane chamber has been removed. Instead, we added a textual description of anesthesia as follow (see at 3:05-3:10 in new version):

“anesthesia : 5% isoflurane in 1L/min oxygen”

We would like to thank you for your understanding and your patience regarding our video and manuscript proposal.

Sincerely yours,

Hélène Castel